Asian Journal of Chemistry; Vol. 28, No. 8 (2016), 1653-1657

ASIAN JOURNAL OF CHEMISTRY

http://dx.doi.org/10.14233/ajchem.2016.19762

Microwave Sol-Gel Derived $PbY_2(MoO_4)_4:Er^{3+}/Yb^{3+}$ Double Molybdate and Their Up-Converted Optical Properties

CHANG SUNG LIM

Department of Advanced Materials Science & Engineering, Hanseo University, Seosan 356-706, Republic of Korea

Corresponding author: Tel/Fax: +82 41 6601445; E-mail: cslim@hanseo.ac.kr

Received: 7 December 2015; *Accepted*: 28 February 2016; *Published online*: 30 April 2016; AJC-17868

$PbY_{2-x}(MoO_4)_4:Er^{3+}/Yb^{3+}$ double molybdate phosphors with the correct doped concentrations of Er^{3+} and Yb^{3+} ($x = Er^{3+} + Yb^{3+}$, $Er^{3+} = 0$, 0.05, 0.1, 0.2 and $Yb^{3+} = 0$, 0.2, 0.45) were precisely prepared using the sol-gel method assisted by the microwave technique; their up-converted optical properties were studied. The particles showed well-crystallized morphology after heat-treated at 900 °C for 16 h. They had a homogeneous and fine morphology with grain sizes of 2-5 μm. After excitation at 980 nm, the $PbY_{1.7}(MoO_4)_4:Er_{0.1}/Yb_{0.2}$ and $PbY_{1.5}(MoO_4)_4:Er_{0.05}/Yb_{0.45}$ double molybdates provided a strong up-converted emission band of 525 nm, a weak up-converted emission band of 550 nm in the green region and a very weak up-converted emission band of 655 nm in the red region. The spectroscopic spectra of Raman for the doped molybdates showed the presence of strong peaks at higher and lower frequencies. It was induced by highly modulated structures of $PbY_{2-x}(MoO_4)_4$ by the incorporation of the Er^{3+} and Yb^{3+} ions into the crystal lattice. These results were attributed to the unit cell shrinkage as well as the anion deficient of the MoO_{4-x} group.

Keywords: Up-converted photoluminescence, $PbY_{2-x}(MoO_4)_4:Er^{3+}/Yb^{3+}$, Microwave, Sol-gel, Raman spectroscopy.

INTRODUCTION

Scheelite-structured compounds belonging to the molybdate family have attracted great application due to their unique spectroscopic properties and dramatically excellent up-converted (UC) optical properties [1]. These up-converted characteristics of the double molybdtaes have current applications in many fields, including optoelectronic devices and luminescence imaging, due to their excellent up-converted luminescencet behaviours. They could overcome the present limitations and enhance the applications of the traditional photoluminescence materials [2,3]. The structure of the molybdate compounds can be transformed to a highly disordered tetragonal Scheelite-type structure from the structure of monoclinic. The trivalent lanthanide ions are partially substituted into the crystal lattices of the Scheelite-type tetragonal phase. The possible doping could be attributed to the similar radii of the trivalent lanthanide ions and bring to the excellent up-converted photoluminescence properties [4-6]. Many lanthanide doping materials such as Er^{3+}, Tm^{3+} and Ho^{3+} are employed as an activator in luminescent centers because of their unique electronic energy levels. The Yb^{3+} ion as a sensitizer can enhance the up-converted luminescence through energy transfer due to its strong absorption around 980 nm. Especially, the co-doped Yb^{3+}/Er^{3+} ions can dramatically enhance the up-converted efficiency through the energy transfer from Yb^{3+} to Er^{3+} [7-9].

To prepare the double molybdates, several processes have been prepared by the specific methods such as solid-state reactions [9-14], co-precipitation [15,16], the sol-gel process [4-7], the hydrothermal method [17,18], the Pechini method [19,20], thermal decomposition [21] and the hydrothermal method assisted by the microwave [22]. Compared to the usual methods, the microwave sol-gel process is an effective method that provides well defined morphology and is easy to proceed. It represent as a effective process for the available synthesis of highly qualified up-converted photoluminescent materials [23-26].

In the present work, $PbY_{2-x}(MoO_4)_4:Er^{3+}/Yb^{3+}$ double molybdate phosphors with the correct doped concentrations of Er^{3+} and Yb^{3+} ($x = Er^{3+} + Yb^{3+}$, $Er^{3+} = 0$, 0.05, 0.1, 0.2 and $Yb^{3+} = 0$, 0.2, 0.45) were synthesized using the sol-gel method assisted by microwave. The phase identification and morphology of the synthesized particles were characterized by X-ray diffraction and scanning electron microscopy. Pump power dependence and Commission Internationale de L'Eclairage (CIE) chromaticity of the up-converted emission intensity were also evaluated. The spectroscopic properties were investigated comparatively using photoluminescence emission as well as Raman spectroscopy.

EXPERIMENTAL

In this study, precise amounts of $Pb(NO_3)_2$, $Y(NO_3)_3{\cdot}6H_2O$, $(NH_4)_6Mo_7O_{24}{\cdot}4H_2O$, $Er(NO_3)_3{\cdot}5H_2O$, $Yb(NO_3)_3{\cdot}5H_2O$, citric acid, NH_4OH, ethylene glycol and distilled water were used to prepare $PbY_2(MoO_4)_4$, $PbY_{1.8}(MoO_4)_4{:}Er_{0.2}$, $PbY_{1.7}(MoO_4)_4{:}Er_{0.1}Yb_{0.2}$ and $PbY_{1.5}(MoO_4)_4Er_{0.05}Yb_{0.45}$ compounds with the correct doped concentrations of Er^{3+} and Yb^{3+} (Er^{3+} = 0, 0.05, 0.1, 0.2 and Yb^{3+}= 0, 0.2, 0.45). For the preparation of the compounds, initially $Pb(NO_3)_2$ and $(NH_4)_6Mo_7O_{24}{\cdot}4H_2O$ were used and dissolved in 80 mL of 5 M NH_4OH with 20 mL of ethylene glycol and under vigorous stirring and heating. Secondly, the lanthanide $Y(NO_3)_3{\cdot}6H_2O$ with the rare-earth containing $Er(NO_3)_3{\cdot}5H_2O$, $Yb(NO_3)_3{\cdot}5H_2O$ were dissolved in 100 mL of distilled water under vigorously heating. At this stage, the citric acid was employed with a molar ratio of citric acid to total metal ions of 2:1. Then, the two kind of solutions were co-mixed together vigorously heated at 80-100 °C. Finally, highly transparent solutions were appeared and treated by the adjusting to pH = 7-8 using the addition of NH_4OH or citric acid. The transparent solutions were moved into a microwave oven. The microwave operations were conducted by the precise controlling with a frequency of 2.45 GHz with a maximum output-power of 1250 W for 30 min. After the microwave process, the samples were dried at 120 °C in a dry oven and black dried gels were obtained. For the crystallization of the compounds, the black dried gels were heat-treated at 900 °C for 16 h. Finally, the pure $PbMoO_4$ as white particles were obtained and the doped compositions as pink particles were obtained

For the phase identifications of the synthesized particles, XRD (D/MAX 2200, Rigaku, Japan) was used. For observation of the surface morphology of the synthesized particles, SEM/EDS (JSM-5600, JEOL, Japan) was used. The up-converted photoluminescnece spectra were measured using a spectrophotometer (Perkin Elmer LS55, UK) at room temperature. Pump power dependence of the measured up-converted emission intensity was evaluated at levels of working current from 20 to 110 mW. Raman spectra measurements were conducted using a LabRam Aramis (Horiba Jobin-Yvon, France). The 514.5 nm line of an Ar ion laser was used as an Raman excitation source. To avoid sample decomposition, the samples were exposed to a power level that was maintained at 0.5 mW.

RESULTS AND DISCUSSION

Fig. 1 shows the XRD patterns of the (a) JCPDS 44-1486 pattern of $PbMoO_4$, the synthesized double molybdates of (b) $PbY_2(MoO_4)_4$, (c) $PbY_{1.8}(MoO_4)_4{:}Er_{0.2}$, (d) $PbY_{1.7}(MoO_4)_4{:}Er_{0.1}/Yb_{0.2}$ and (e) $PbY_{1.5}(MoO_4)_4Er_{0.05}/Yb_{0.45}$ particles. The crystal structures are identified with the crystallographic data of $PbMoO_4$ (JCPDS 44-1486). The pure $PbMoO_4$ is a Scheelite-type tetragonal structure with space group $I4_1/a$ and the major crystal planes of wulfenite $PbMoO_4$ match well with (112), (204) and (312) at 17.8°, 27.5° and 55.6°. The $PbMoO_4$ has the optimized cell parameters of a = 5.511 Å and c = 12.346 Å. The predict bond lengths of Mo-O in MoO_4 tetrahedral are 1.800 Å and the nearest distance of Pb-O is about 2.655 Å [27]. The XRD patterns of (b) $PbY_2(MoO_4)_4$, (c) $PbY_{1.8}(MoO_4)_4{:}Er_{0.2}$ and (d) $PbY_{1.7}(MoO_4)_4{:}Er_{0.1}/Yb_{0.2}$ particles showed no impurity phases. In Fig. 1(e), the impurity phases were detected at 18.5°, 25°, 26°, 31°, 34°, 35°, 48°, 49° and 49.5° as can be seen. When the doping concentration of 0.02 mol % Er^{3+} and 0.18 mol % Yb^{3+}, the marked foreign reflexes observed with an asterisk in Fig. 1(e). The secondary phases are assumed to be one of the MoO_{4-x} groups (MoO_3, Mo_4O_{11}, Mo_8O_{23} and Mo_9O_{26}). However, the identification of the secondary phases is very difficult, because very weak peaks are observed. The MoO_{4-x} groups have similar XRD patterns and complicated reflexes. In the case of Er^{3+}/Yb^{3+} doped co-doped $CaLa_2(MoO_4)_4$ phosphor, a similar impurity phase was also observed when the doping concentration of 0.02 mol % Er^{3+} and 0.18 mol % Yb^{3+}[25]. The foreign reflexes in Fig. 1(e) can be ascribed that Er^{3+} and Yb^{3+} ions could be well substituted in the $PbY_2(MoO_4)_4$ tetragonal-phase of the Scheelite-type structure. It forms a new disordered phase by the incorporation of the Er^{3+} and Yb^{3+} elements into the $PbY_2(MoO_4)_4$ crystal lattice. This result gives rise to the unit cell shrinkage with the highly modulated MoO_{4-x} group [25-27].

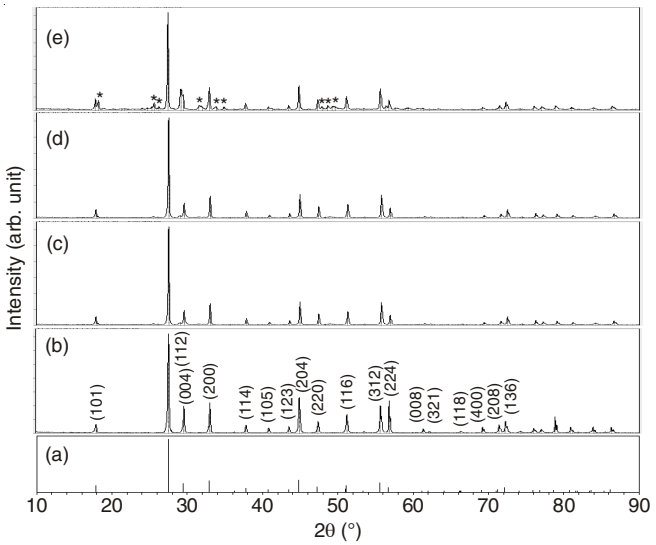

Fig. 1. XRD patterns of (a) JCPDS 44-1486 pattern of $PbMoO_4$ and the synthesized (b) $PbY_2(MoO_4)_4$, (c) $PbY_{1.8}(MoO_4)_4{:}Er_{0.2}$, (d) $PbY_{1.7}(MoO_4)_4{:}Er_{0.1}/Yb_{0.2}$ and (e) $PbY_{1.5}(MoO_4)_4Er_{0.05}YYb_{0.45}$ particles

The unit cell shrinkage could be resulted by the substitution of Y^{3+} ions by Er^{3+} and Yb^{3+} ions. This result accompanies the highly modulated structure induced by the anion deficient MoO_{4-x} group. This incommensurately modulated structures in the Scheelite-type tetragonal phase were also observed in various molybdates and tungstates as a cation deficient structure [28-30]. Previously, our research group has reported the incommensurately modulated structure of $CaGd_2(WO_4)_4{:}Er^{3+}/Yb^{3+}$ phosphors induced by the difference of effective ionic radii of Yb^{3+}, Er^{3+} and Gd^{3+} [31].

Fig. 2 shows SEM images of the as-synthesized (a) $PbY_2(MoO_4)_4$ and (b) $PbY_{1.5}(MoO_4)_4Er_{0.05}/Yb_{0.45}$ particles. The particles showed well-crystallized morphology after heat-treated at 900 °C for 16 h. They had a homogeneous and fine morphology with grain sizes of 2-5 μm. The samples have no

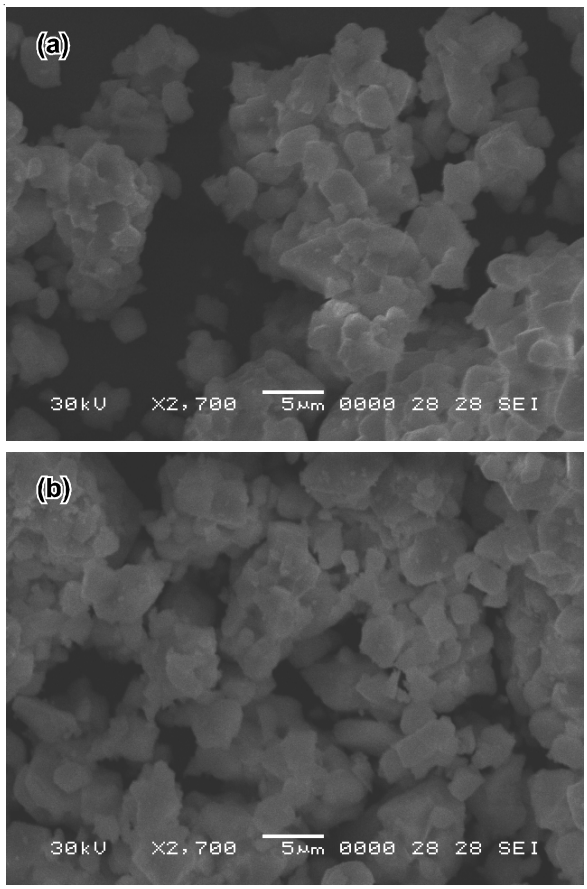

Fig. 2. SEM images of the (a) $PbY_2(MoO_4)_4$ and (b) $PbY_{1.5}(MoO_4)_4Er_{0.05}/Yb_{0.45}$ particles

discrepancy in aspect of morphological feature and some agglomerated particles induced by the inter-diffusions among the grains. It is noted that the doped concentrations for Er^{3+} and Yb^{3+} have no effects on the apparent morphological feature. The microwave sol-gel method of the double molybdate provides the fine particles, which can be prepared in a short time period. This process is a cost-effective method to fabricate highly fine products for the suitable up-converted particles.

Fig. 3 shows the up-converted photoluminescence emission spectra of the as-prepared (a) $PbY_2(MoO_4)_4$, (b) $PbY_{1.8}(MoO_4)_4:Er_{0.2}$, (c) $PbY_{1.7}(MoO_4)_4:Er_{0.1}/Yb_{0.2}$ and (d) $PbY_{1.5}(MoO_4)_4:Er_{0.05}/Yb_{0.45}$ particles excited under 980 nm at room temperature. The (c) $PbY_{1.7}(MoO_4)_4:Er_{0.1}/Yb_{0.2}$ and (d) $PbY_{1.5}(MoO_4)_4:Er_{0.05}/Yb_{0.45}$ particles exhibited a strong up-converted emission band of 525 nm, a weak up-converted emission band of 550 nm in the green region and a very weak up-converted emission band of 655 nm in the red region. The strong up-converted emission band of 525 nm and the weak up-converted emission band of 550 nm in the green region correspond to the transitions of $^2H_{11/2} \rightarrow {}^4I_{15/2}$ and $^4S_{3/2} \rightarrow {}^4I_{15/2}$, respectively. The very weak up-converted emission band of 655 nm in the red region corresponds to the transition of $^4F_{9/2} \rightarrow {}^4I_{15/2}$. The (a) $PbY_2(MoO_4)_4$ and (b) $PbY_{1.8}(MoO_4)_4:Er_{0.2}$ particles exhibited very weak up-converted emission bands of 525 nm and 550 nm in the green region. The up-converted intensity of (d) $PbY_{1.5}(MoO_4)_4:Er_{0.05}/Yb_{0.45}$ showed much higher value compared to that of (c) $PbY_{1.7}(MoO_4)_4:Er_{0.1}/Yb_{0.2}$. In other host matrices, similar results are also appeared from

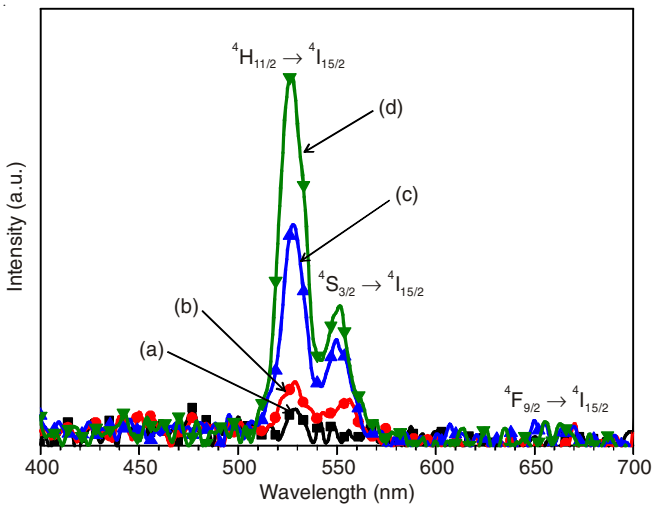

Fig. 3. Up-converted photoluminescence emission spectra of (a) $PbY_2(MoO_4)_4$, (b) $PbY_{1.8}(MoO_4)_4:Er_{0.2}$, (c) $PbY_{1.7}(MoO_4)_4:Er_{0.1}/Yb_{0.2}$ and (d) $PbY_{1.5}(MoO_4)_4Er_{0.05}/Yb_{0.45}$ particles excited under 980 nm at room temperature

Er^{3+}/Yb^{3+} co-doped systems, which are corresponded to the up-converted emission spectra with the green up-converted emission intensity $^2H_{11/2} \rightarrow {}^4I_{15/2}$ and $^4S_{3/2} \rightarrow {}^4I_{15/2}$ and the red up-converted emission intensity for the transitions of $^4F_{9/2} \rightarrow {}^4I_{15/2}$ [7,10,25,26].

In Fig. 4, the logarithmic scale dependence for the obtained up-converted emission intensities at 525, 550 and 655 nm on the working pump power over the range of 20 to 110 mW in the $PbY_{2-x}(MoO_4)_4:Er^{3+}/Yb^{3+}$ sample is shown. In the up-converted process, the intensity of up-converted emission is proportional to the slope value n of the irradiation pumping power, where n is the number of pumped photons required to produce up-converted emission [32].

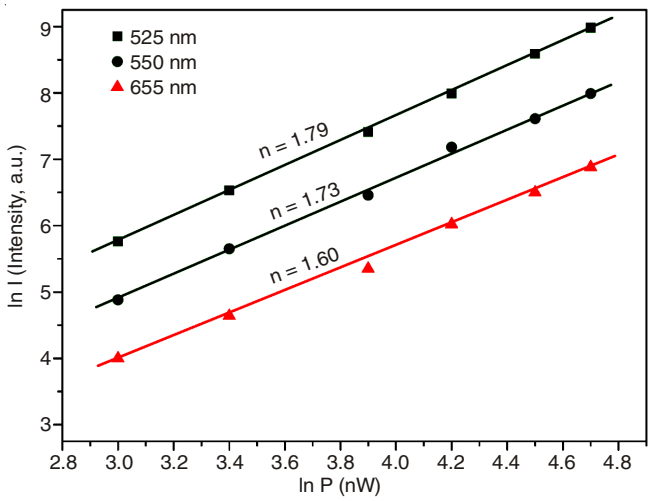

Fig. 4. Logarithmic scale of pump power dependence of the up-converted emission intensity on the working current from 20 to 110 mW at 525, 550 and 655 nm in the $PbY_{2-x}(MoO_4)_4:Er^{3+}/Yb^{3+}$ system

$$I \propto P^n$$

$$\ln I \propto n \ln P$$

where the value n is the number of the pumped photons, which are required to excite the upper emitting state. I is the up-converted luminescent intensity and P is the laser pumping

power. The calculated slope value n, shown in Fig. 4, indicate a slope n = 1.79 and 1.73 for green emission at 525 and 550 nm and 1.60 for red emission at 655 nm. These results indicate that the up-converted mechanism of the green and red emissions can be ascribed by a two-photon process in Er^{+3}/Yb^{3+} co-doped $PbY_{2-x}(MoO_4)_4$ phosphors [14-18].

Fig. 5 shows (A) calculated chromaticity coordinate (x, y) values and (B) CIE chromaticity diagram for (a) $PbY_2(MoO_4)_4$, (b) $PbY_{1.8}(MoO_4)_4:Er_{0.2}$, (c) $PbY_{1.7}(MoO_4)_4:Er_{0.1}/Yb_{0.2}$ and (d) $PbY_{1.5}(MoO_4)_4:Er_{0.05}/Yb_{0.45}$ particles. The indicated triangle in Fig. 5(b) is the standard colour coordinates for blue, green and red. The insets in Fig. 5(b) show the chromaticity points for the samples (a), (b), (c) and (d). When the concentration ratios of Er^{3+}/Yb^{3+} are modulated, the chromaticity coordinate values (x, y) change. As can be seen in Fig. 5, the calculated chromaticity coordinates x = 0.312 and y = 0.486 for (c) $PbY_{1.7}(MoO_4)_4:Er_{0.1}Yb_{0.2}$ and x = 0.308 and y = 0.523 for (d) $PbY_{1.5}(MoO_4)_4:Er_{0.05}Yb_{0.45}$ correspond to yellowish green emissions and the standard equal energy point in the CIE diagram.

The Raman spectrum of the $PbY_2(MoO_4)_4$ crystal in Fig. 6(a) shows the typical molybdate compounds, which is shown as two divided parts with a wide empty gap of 360-740 cm^{-1}. The highest wavenumber band at 870 cm^{-1} corresponds to stretching vibrations of the MoO_4. The stretching vibrations of Mo-O bonds are observed in the 746 and 772 cm^{-1} regions. For these stretching vibrations, strong mixing occurs between the Mo-O bonds and the MoO_4 polyhedron. The band at 320 and 354 cm^{-1} could be assumed to originate from vibrations of the longer Mo-O bonds, which are employed in the formation of the Mo-Mo bridge. The translational vibration motion of the Y-O bonds is observed at 172 cm^{-1}, which is located at levels lower than 180 cm^{-1}. The Raman spectra of (b) $PbY_{1.8}(MoO_4)_4:Er_{0.2}$, (c) $PbY_{1.7}(MoO_4)_4:Er_{0.1}/Yb_{0.2}$ and (d) $PbY_{1.5}(MoO_4)_4:Er_{0.05}/Yb_{0.45}$ particles show the very strong and dominant peaks at higher frequencies of 871, 1033, 1090 and 1300 cm^{-1} and at lower frequencies of 230, 368, 418 and 555 cm^{-1}. These strong peaks at higher and lower frequencies are attributed to the disordered structures of $PbY_{2-x}(MoO_4)_4$ by the incorporation of the Er^{3+} and Yb^{3+} ions into the host crystal lattice, which result in the unit cell shrinkage as well as the highly modulated MoO_{4-x} group. These results provide the highly emitted efficiency with stable thermal and chemical properties. These up-converted double molybdate materials can overcome the current limitations of traditional luminescence phodphors. It can be considered potentially active new up-converted phosphors in new optoelectronic devices and in photoluminescent imaging.

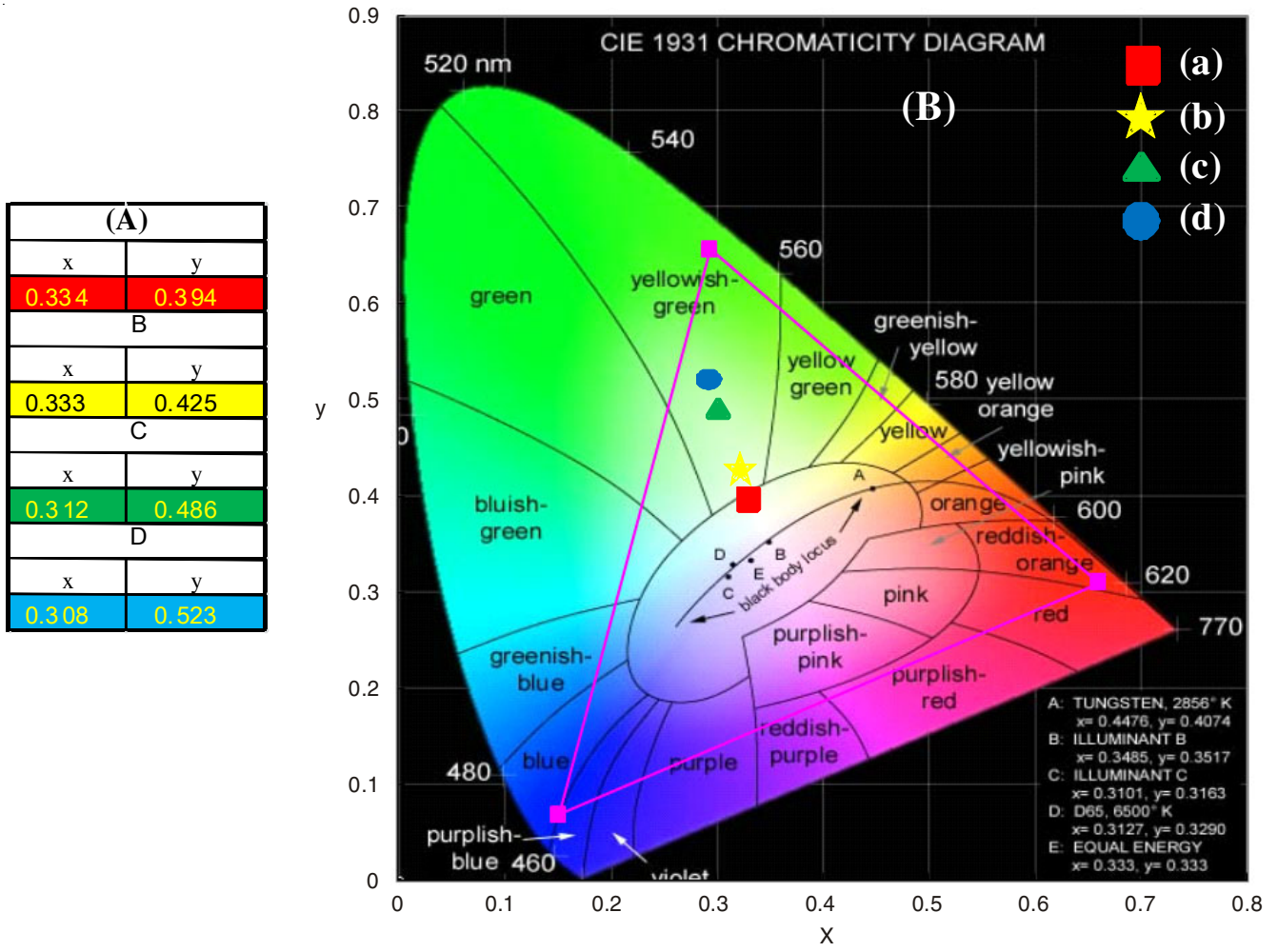

Fig. 5. (A) Calculated chromaticity coordinate (x, y) values and (B) CIE chromaticity diagram for (a) $PbY_2(MoO_4)_4$, (b) $PbY_{1.8}(MoO_4)_4:Er_{0.2}$, (c) $PbY_{1.7}(MoO_4)_4:Er_{0.1}/Yb_{0.2}$ and (d) $PbY_{1.5}(MoO_4)_4Er_{0.05}/Yb_{0.45}$ particles

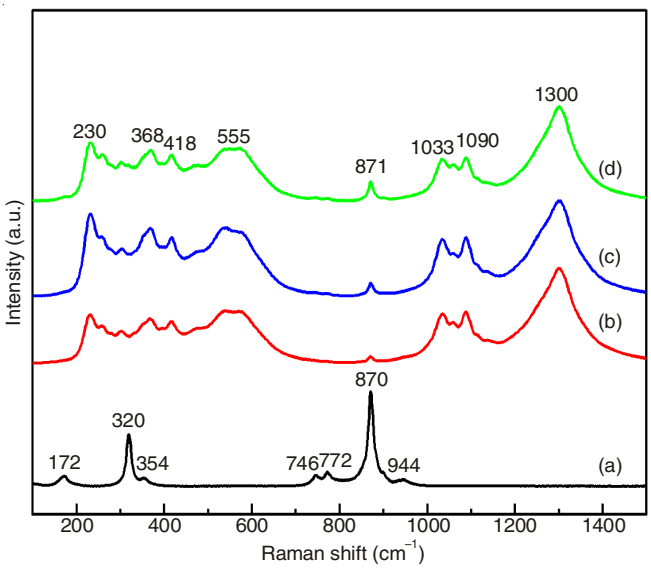

Fig. 6. Raman spectra of the synthesized (a) pure $PbY_2(MoO_4)_4$, (b) $PbY_{1.8}(MoO_4)_4:Er_{0.2}$, (c) $PbY_{1.7}(MoO_4)_4:Er_{0.1}/Yb_{0.2}$ and (d) $PbY_{1.5}(MoO_4)_4Er_{0.05}/Yb_{0.45}$ particles excited by the 514.5 nm line of an Ar ion laser at 0.5 mW

Conclusion

$PbY_{2-x}(MoO_4)_4:Er^{3+}/Yb^{3+}$ double molybdate phosphors with the correct doped concentrations of Er^{3+} and Yb^{3+} were precisely prepared using the sol-gel method assisted by the microwave technique. The particles showed well-crystallized morphology after heat-treated at 900 °C for 16 h. They had a homogeneous and fine morphology with grain sizes of 2-5 μm. After excitation at 980 nm, the $PbY_{1.7}(MoO_4)_4:Er_{0.1}/Yb_{0.2}$ and $PbY_{1.5}(MoO_4)_4:Er_{0.05}/Yb_{0.45}$ double molybdates provided a strong up-converted emission band of 525 nm, a weak up-converted emission band of 550 nm in the green region and a very weak up-converted emission band of 655 nm in the red region. The up-converted emission bands of 525 nm and 550 nm in the green region were corresponded to the transitions of $^2H_{11/2} \rightarrow {}^4I_{15/2}$ and $^4S_{3/2} \rightarrow {}^4I_{15/2}$, while the up-converted emission band of 655 nm in the red region was corresponded to the transition of $^4F_{9/2} \rightarrow {}^4I_{15/2}$. The up-converted intensity of $PbY_{1.5}(MoO_4)_4:Er_{0.05}/Yb_{0.45}$ particles was much higher than that of the $PbY_{1.7}(MoO_4)_4:Er_{0.1}/Yb_{0.2}$ particles. The spectroscopic spectra of Raman for the doped molybdates showed the presence of strong peaks at higher and lower frequencies. It was induced by highly modulated structures of $PbY_{2-x}(MoO_4)_4$ by the incorporation of the Er^{3+} and Yb^{3+} ions into the crystal lattice. These results were attributed by the unit cell shrinkage as well as the anion deficient of the MoO_{4-x} group.

ACKNOWLEDGEMENTS

This research was supported by the Basic Science Research Program through the National Research Foundation of Korea (NRF) funded by the Ministry of Education (2015-058813).

REFERENCES

1. C.S. Lim, A. Aleksandrovsky, M. Molokeev, A. Oreshonkov and V. Atuchin, *Phys. Chem. Chem. Phys.*, **17**, 19278 (2015).
2. M. Lin, Y. Zhao, S.Q. Wang, M. Liu, Z.F. Duan, Y.M. Chen, F. Li, F. Xu and T.J. Lu, *Biotechnol. Adv.*, **30**, 1551 (2012).
3. M.V. DaCosta, S. Doughan, Y. Han and U.J. Krull, *Anal. Chim. Acta*, **832**, 1 (2014).
4. J. Liao, D. Zhou, B. Yang, R. Liu, Q. Zhang and Q. Zhou, *J. Lumin.*, **134**, 533 (2013).
5. J. Sun, Y. Lan, Z. Xia and H. Du, *Opt. Mater.*, **33**, 576 (2011).
6. C. Guo, H.K. Yang and J.H. Jeong, *J. Lumin.*, **130**, 1390 (2010).
7. T. Li, C. Guo, Y. Wu, L. Li and J.H. Jeong, *J. Alloys Comp.*, **540**, 107 (2012).
8. M. Nazarov and D.Y. Noh, *J. Rare Earths*, **28**, 1 (2010).
9. J. Sun, W. Zhang, W. Zhang and H. Du, *Mater. Res. Bull.*, **47**, 786 (2012).
10. H. Du, Y. Lan, Z. Xia and J. Sun, *Mater. Res. Bull.*, **44**, 1660 (2009).
11. Z. Wang, H. Liang, M. Gong and Q. Su, *J. Alloys Comp.*, **432**, 308 (2007).
12. M. Haque and D.K. Kim, *Mater. Lett.*, **63**, 793 (2009).
13. C. Zhao, X. Yin, F. Huang and Y. Hang, *J. Solid State Chem.*, **184**, 3190 (2011).
14. L. Qin, Y. Huang, T. Tsuboi and H.J. Seo, *Mater. Res. Bull.*, **47**, 4498 (2012).
15. Y. Yang, E. Liu, L. Li, Z. Huang, H. Shen and X. Xiang, *J. Alloys Comp.*, **505**, 555 (2010).
16. Y. Tian, B. Chen, B. Tian, R. Hua, J. Sun, L. Cheng, H. Zhong, X. Li, J. Zhang, Y. Zheng, T. Yu, L. Huang and Q. Meng, *J. Alloys Comp.*, **509**, 6096 (2011).
17. Y. Huang, L. Zhou, L. Yang and Z. Tang, *Opt. Mater.*, **33**, 777 (2011).
18. Y. Tian, B. Chen, B. Tian, J. Sun, X. Li, J. Zhang, L. Cheng, H. Zhong, H. Zhong, Q. Meng and R. Hua, *Physica B*, **407**, 2556 (2012).
19. Z. Wang, H. Liang, L. Zhou, J. Wang, M. Gong and Q. Su, *J. Lumin.*, **128**, 147 (2008).
20. Q. Chen, L. Qin, Z. Feng, R. Ge, X. Zhao and H. Xu, *J. Rare Earths*, **29**, 843 (2011).
21. X. Shen, L. Li, F. He, X. Meng and F. Song, *Mater. Chem. Phys.*, **132**, 471 (2012).
22. J. Zhang, X. Wang, X. Zhang, X. Zhao, X. Liu and L. Peng, *Inorg. Chem. Commun.*, **14**, 1723 (2011).
23. S. Das, A.K. Mukhopadhyay, S. Datta and D. Basu, *Bull. Mater. Sci.*, **32**, 1 (2009).
24. T. Thongtem, A. Phuruangrat and S. Thongtem, *J. Nanopart. Res.*, **12**, 2287 (2010).
25. C.S. Lim, *Mater. Res. Bull.*, **60**, 537 (2014).
26. C.S. Lim, *Infrared Phys. Technol.*, **67**, 371 (2014).
27. R.D. Shannon, *Acta Crystallogr. A*, **32**, 751 (1976).
28. A.M. Abakumov, V.A. Morozov, A.A. Tsirlin, J. Verbeeck and J. Hadermann, *Inorg. Chem.*, **53**, 9407 (2014).
29. V.A. Morozov, A. Bertha, K.W. Meert, S. Van Rompaey, D. Batuk, G.T. Martinez, S. Van Aert, P.F. Smet, M.V. Raskina, D. Poelman, A.M. Abakumov and J. Hadermann, *Chem. Mater.*, **25**, 4387 (2013).
30. V.A. Morozov, A.V. Mironov, B.I. Lazoryak, E.G. Khaikina, O.M. Basovich, M.D. Rossell and G. Van Tendeloo, *J. Solid State Chem.*, **179**, 1183 (2006).
31. C.S. Lim, A. Aleksandrovsky, M. Molokeev, A. Oreshonkov and V. Atuchin, *J. Solid State Chem.*, **228**, 160 (2015).
32. H. Guo, N. Dong, M. Yin, W. Zhang, L. Lou and S. Xia, *J. Phys. Chem. B*, **108**, 19205 (2004).